Supporting information for

Single-atom catalysts supported on a hybrid structure of boron nitride/graphene for efficient nitrogen fixation via synergistic interfacial interactions

Mohammad Zafari[1,2], Rohit Anand[1], Arun S. Nissimagoudar[1], Miran Ha[1], Geunsik Lee[1,2]*, Kwang S. Kim[1]*

[1]Center for Superfunctional Materials, Department of Chemistry, Ulsan National Institute of Science and Technology (UNIST), 50 UNIST-gil, Ulsan 44919, Republic of Korea

[2]Center for Multidimensional Carbon Materials (CMCM), Institute for Basic Science (IBS), Ulsan 44919, Republic of Korea

*Corresponding authors: gslee@unist.ac.kr, kimks@unist.ac.kr

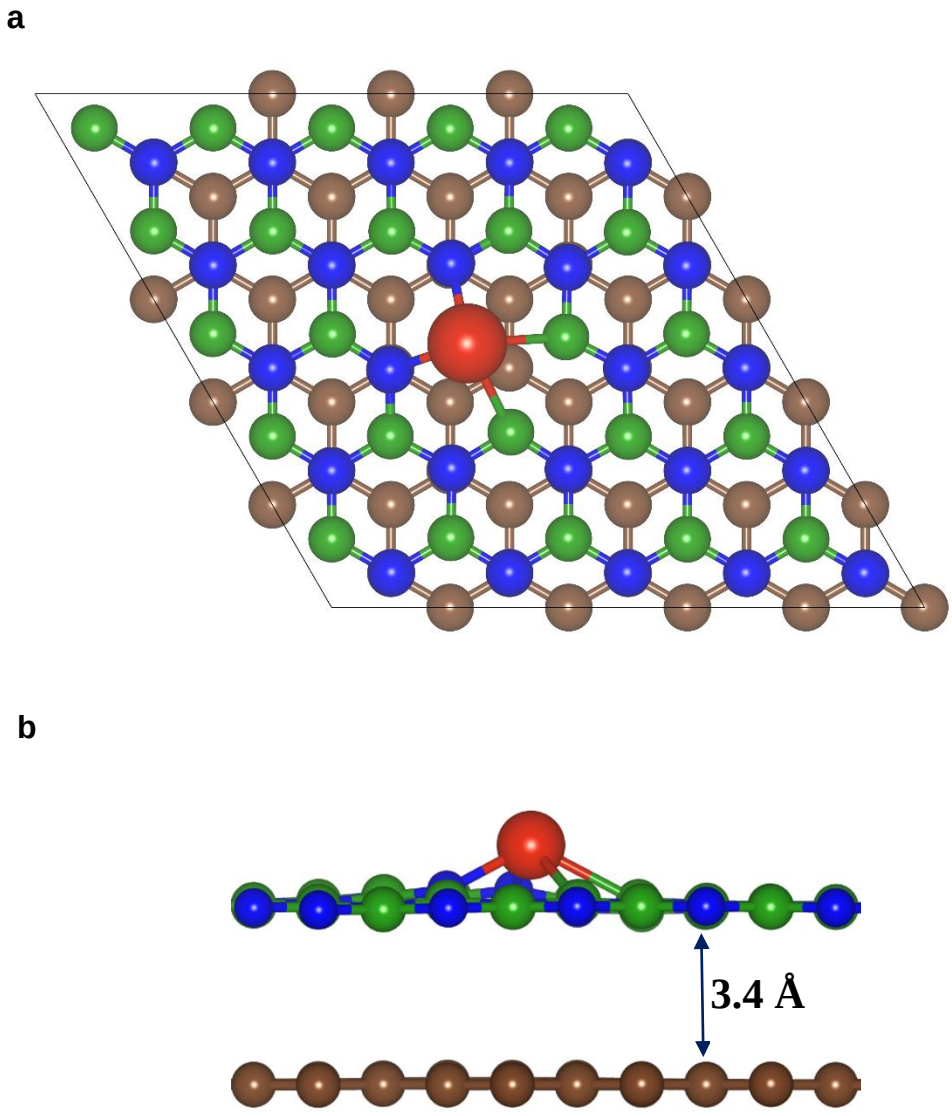

Figure S1. (a) Top view of transition metal (TM) doped into BN/G hybrid structure in which double B and N vacancies were created for embedding TM. (b) Front view of the hybrid structure single atom catalyst. The interlayer distance is around 3.4 Å and TM was surrounded with B_2N_2. Color code, TM: Red, nitrogen: blue, boron: green, carbon: brown.

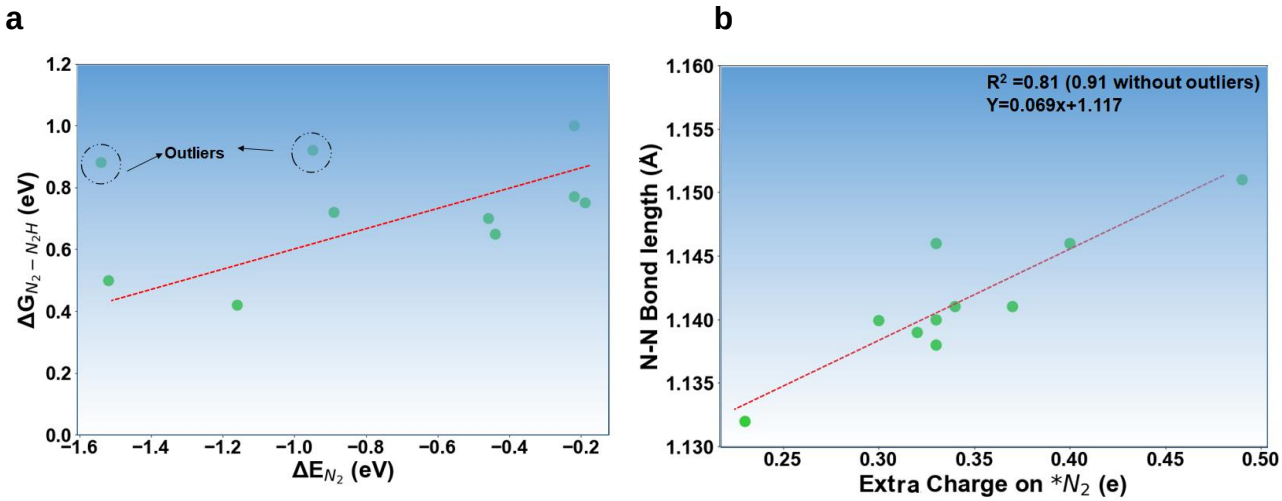

Figure S2. (a) Free energy changes of the first pronation step ($*N_2$ to $*N_2H$) versus adsorption energy of $*N_2$. (b) N-N bond elongation as a function of extra charge on adsorbed $*N_2$.

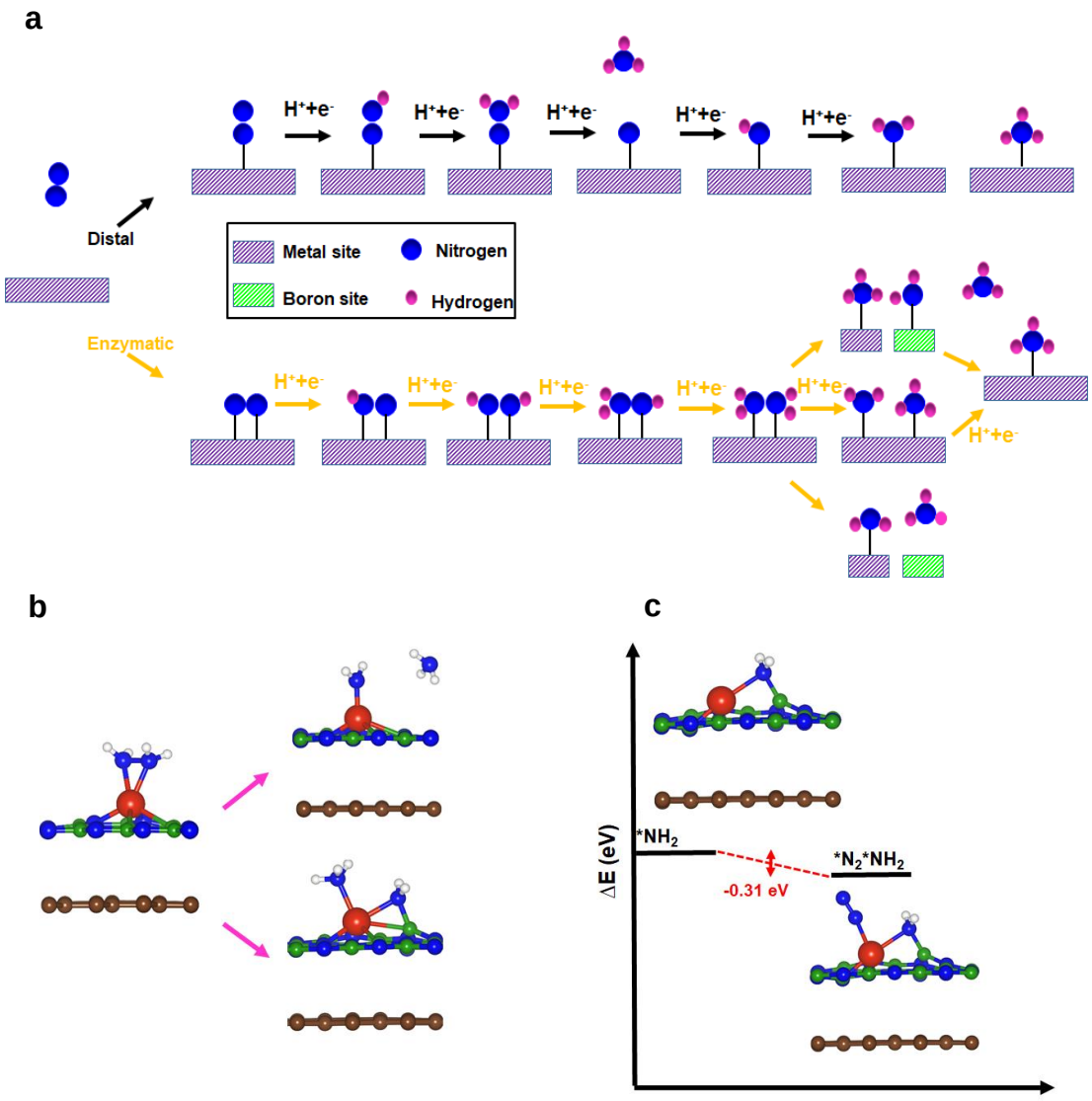

Figure S3. (a) Possible NRR reaction paths of BN/G SACs through the associative mechanism. (b) Two main intermediate species after $*NH_2$-$*NH_2$ formation for releasing the first ammonia via an enzymatic pathway and (c) adsorption energy of N_2 on V-SAC after releasing ammonia.

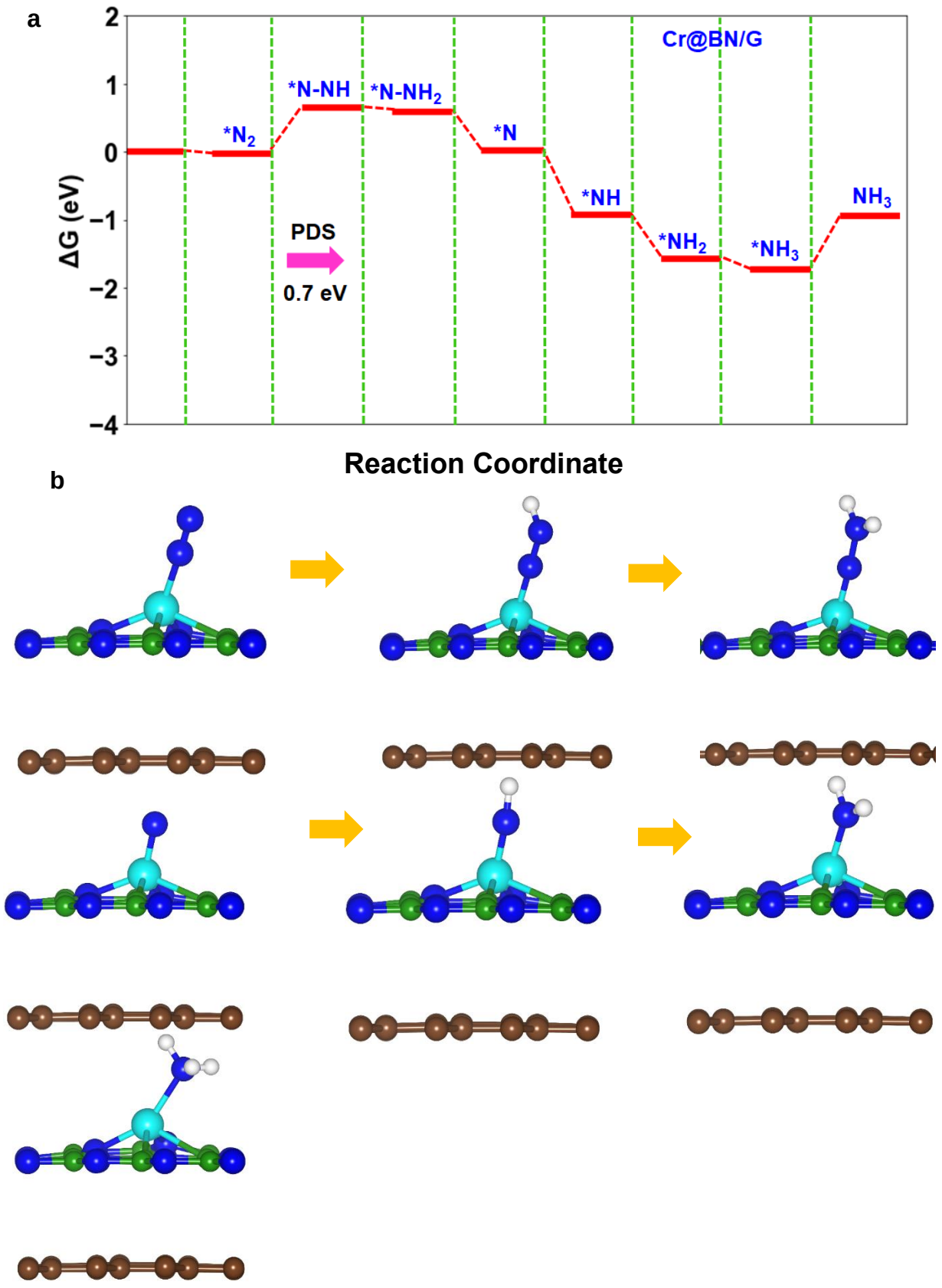

Figure S4. (a) Free energy diagram for N_2 reduction to NH_3 on Cr-doped BN/G SAC via distal mechanism and (b) its adsorption structures during the NRR reaction.

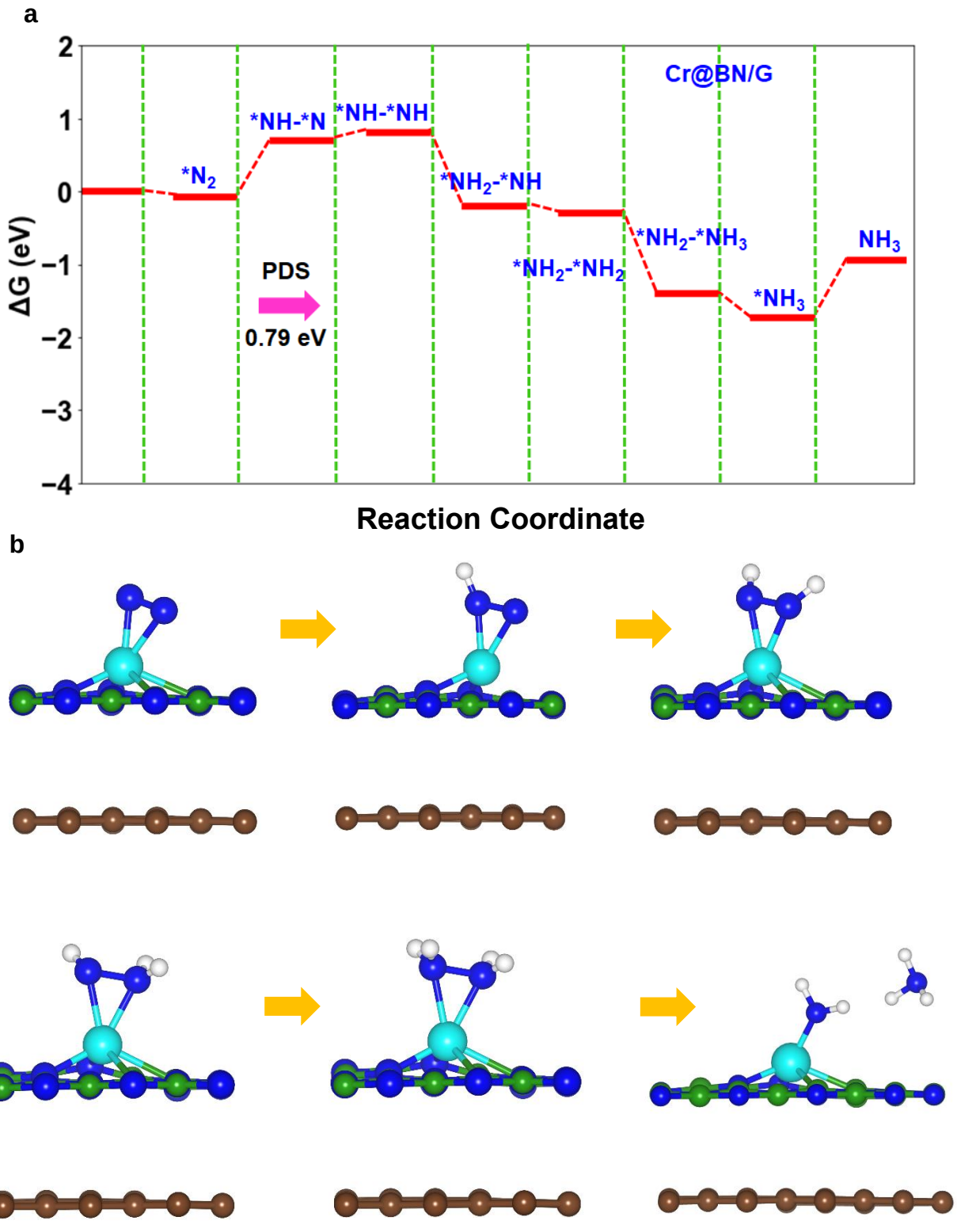

Figure S5. (a) Free energy diagram for N_2 reduction to NH_3 on Cr-doped BN/G SAC via enzymatic mechanism and (b) its adsorption structures during the NRR reaction.

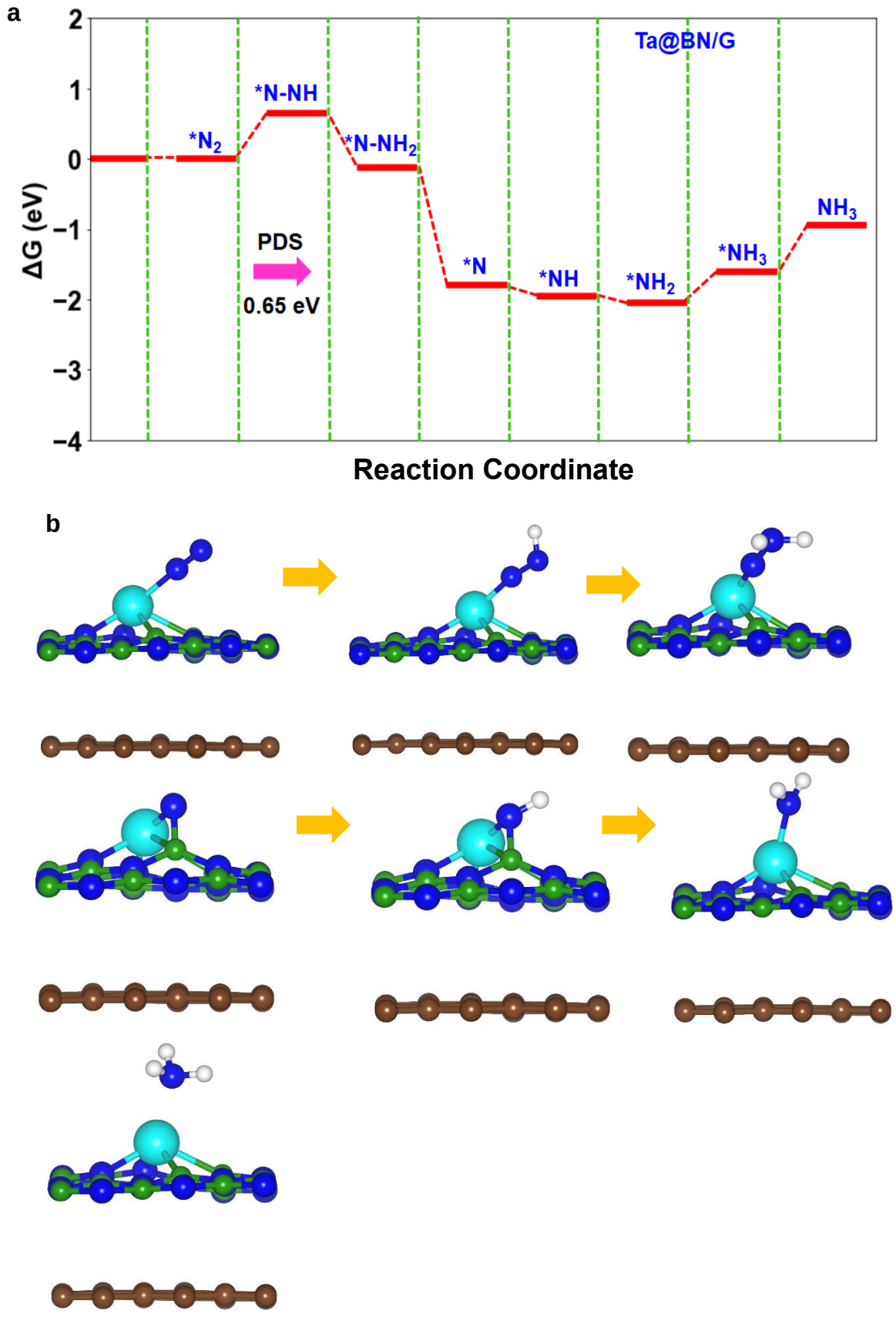

Figure S6. (a) Free energy diagram for N_2 reduction to NH_3 on Ta-doped BN/G SAC via distal mechanism and (b) its adsorption structures during the NRR reaction.

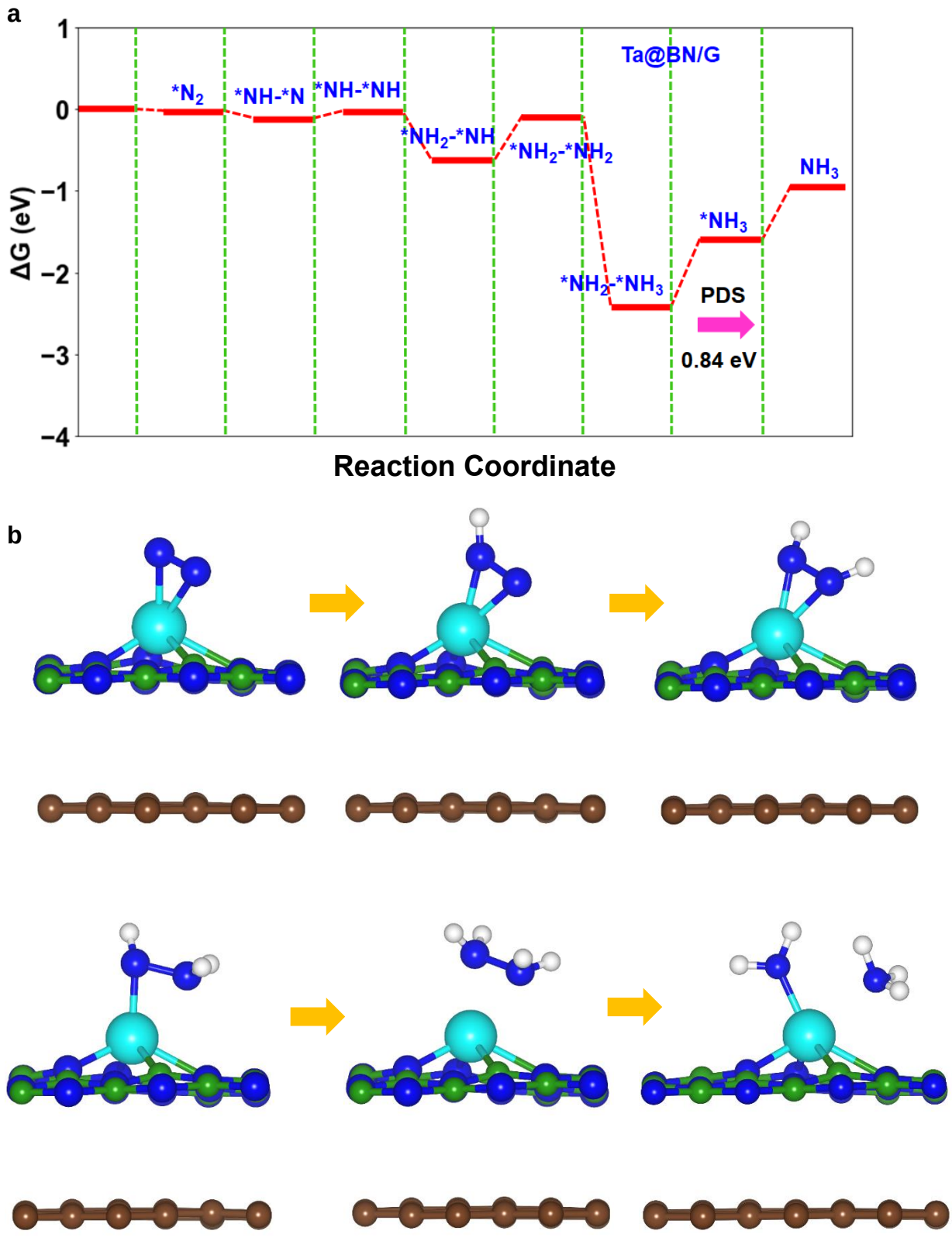

Figure S7. (a) Free energy diagram for N_2 reduction to NH_3 on Ta-doped BN/G SAC via enzymatic mechanism and (b) its adsorption structures during the NRR reaction.

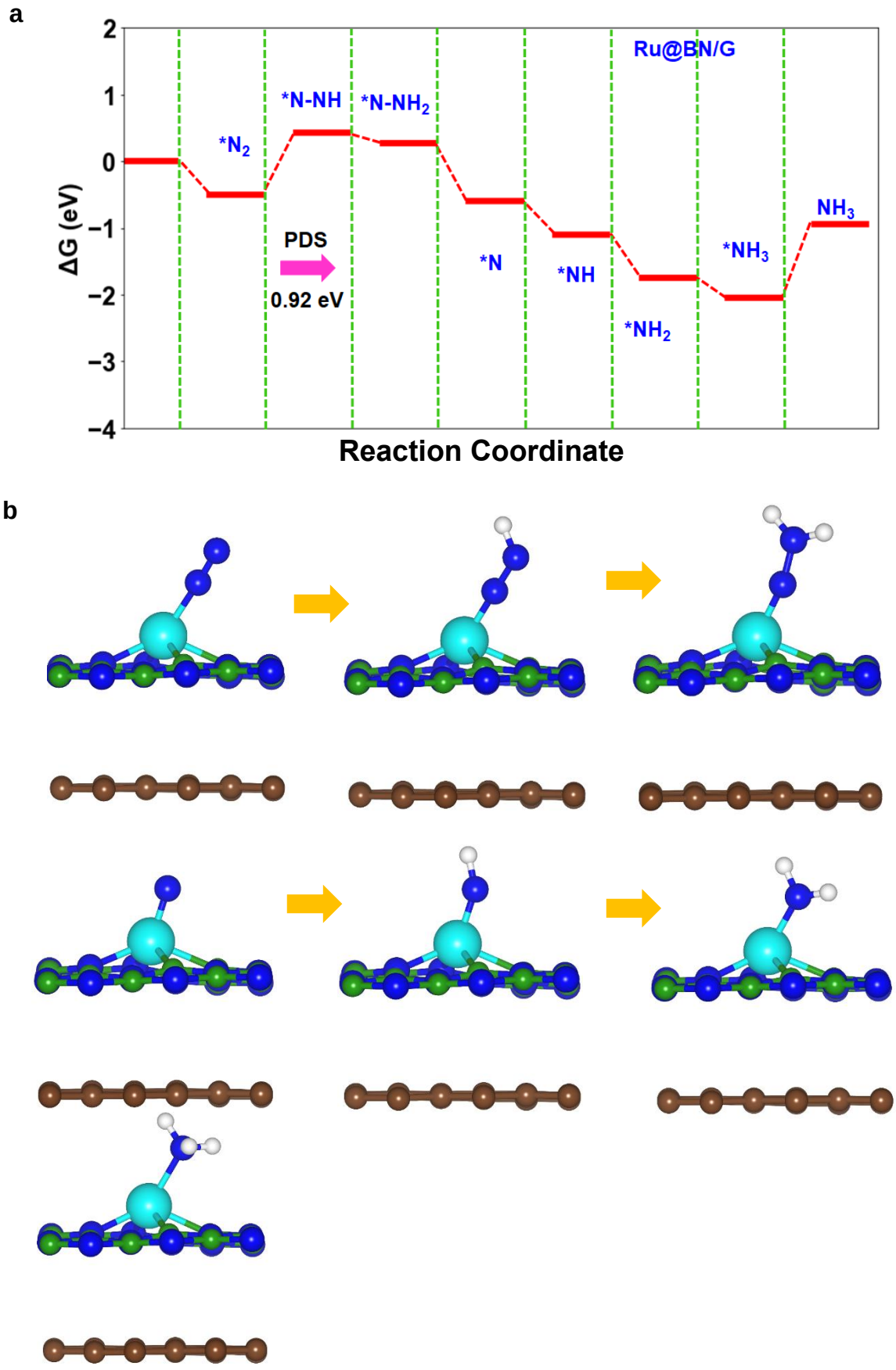

Figure S8. (a) Free energy diagram for N_2 reduction to NH_3 on Ru-doped BN/G SAC via distal mechanism and (b) its adsorption structures during the NRR reaction.

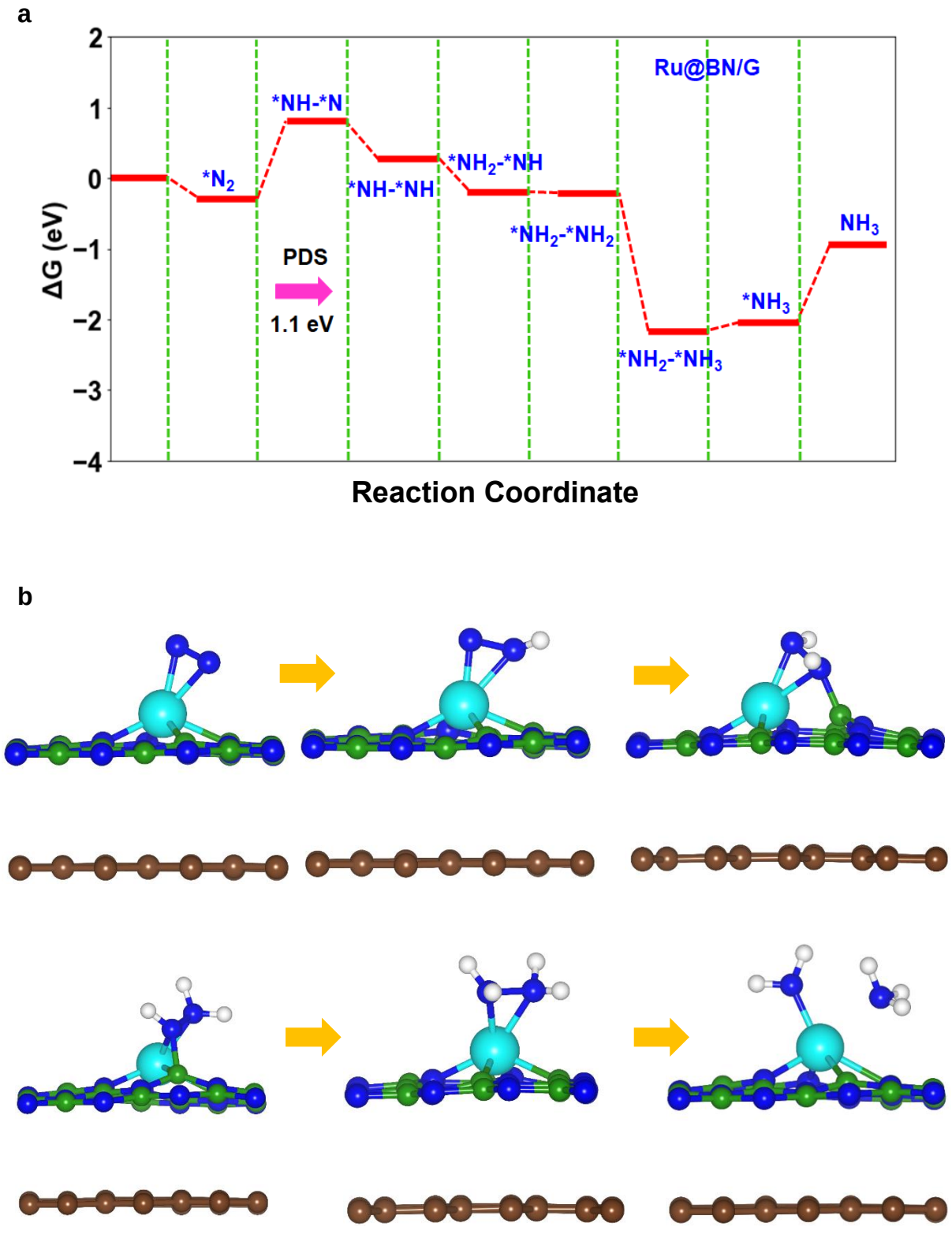

Figure S9. (a) Free energy diagram for N_2 reduction to NH_3 on Ru-doped BN/G SAC via enzymatic mechanism and (b) its adsorption structures during the NRR reaction.

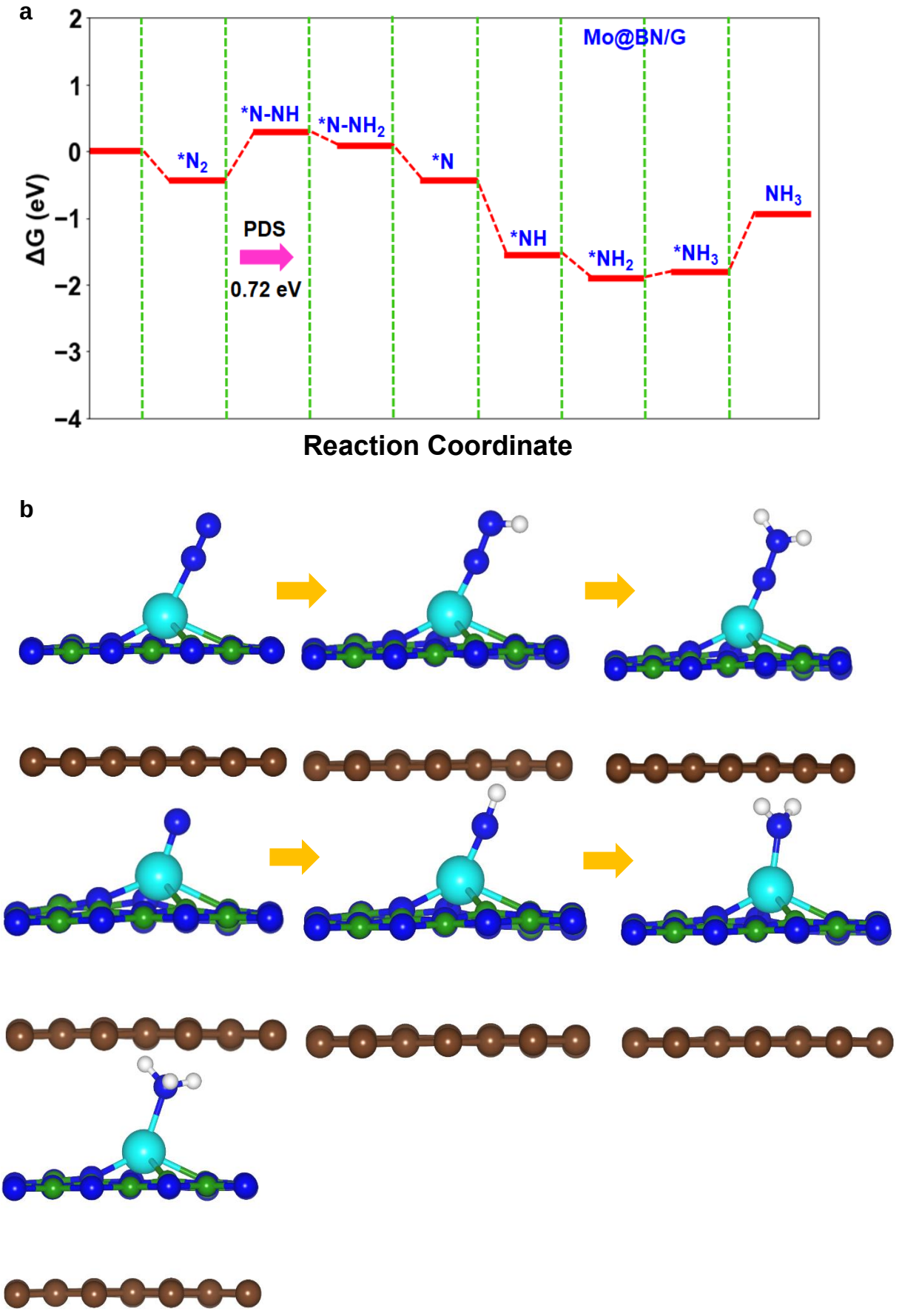

Figure S10. (a) Free energy diagram for N_2 reduction to NH_3 on Mo-doped BN/G SAC via distal mechanism and (b) its adsorption structures during the NRR reaction.

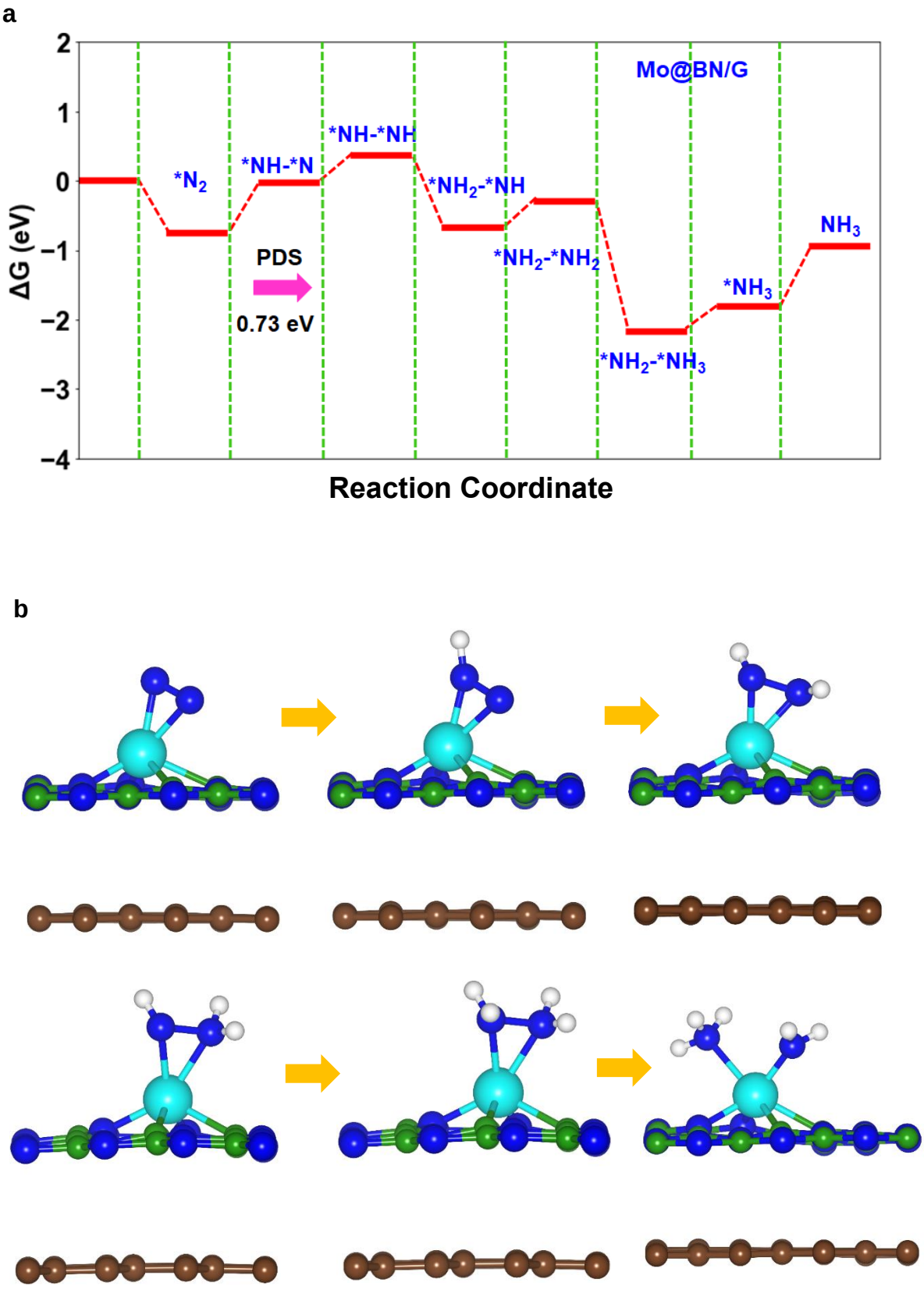

Figure S11. (a) Free energy diagram for N_2 reduction to NH_3 on Mo-doped BN/G SAC via enzymatic mechanism and (b) its adsorption structures during the NRR reaction.

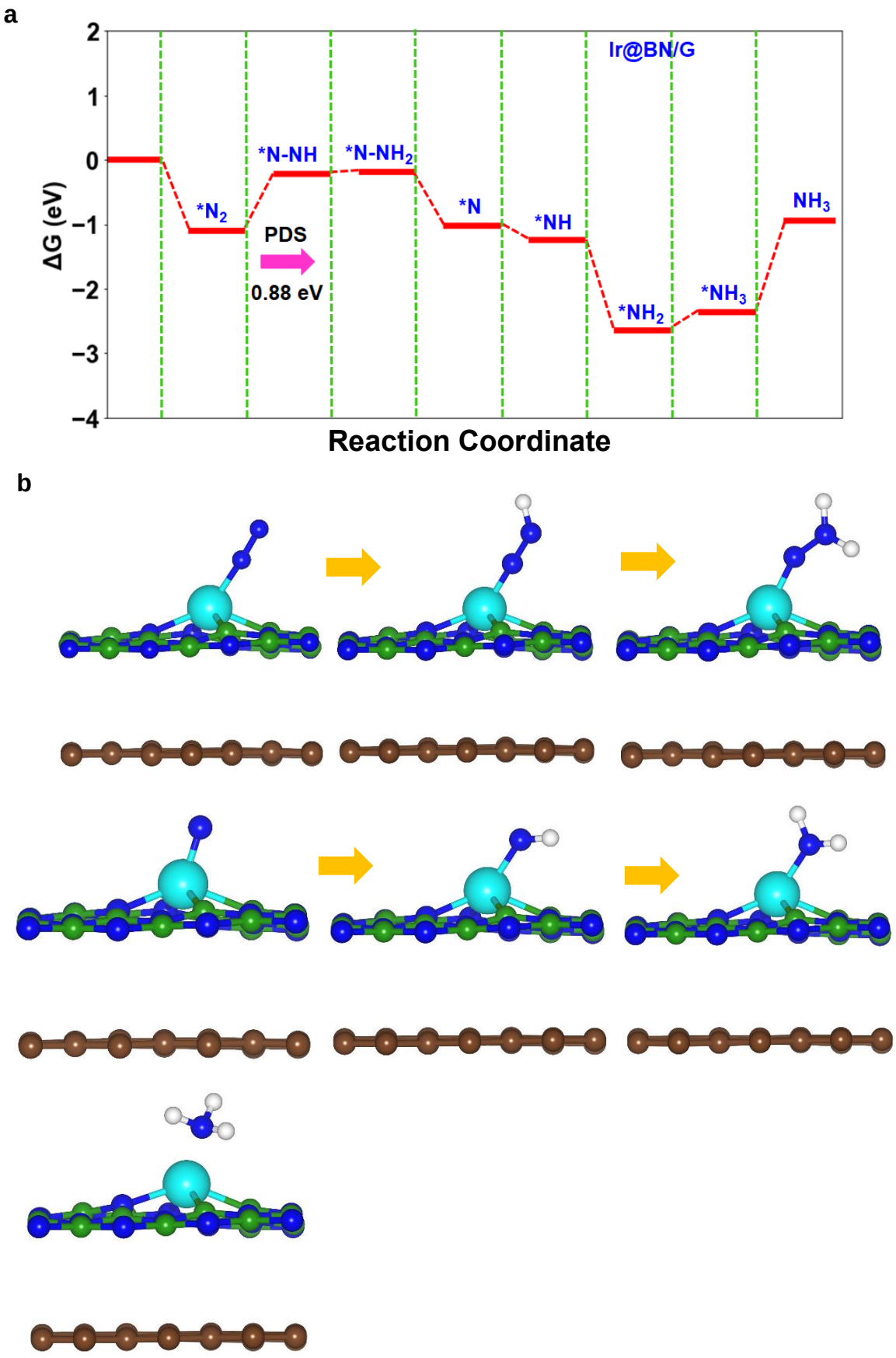

Figure S12. (a) Free energy diagram for N_2 reduction to NH_3 on Ir-doped BN/G SAC via distal mechanism and (b) its adsorption structures during the NRR reaction.

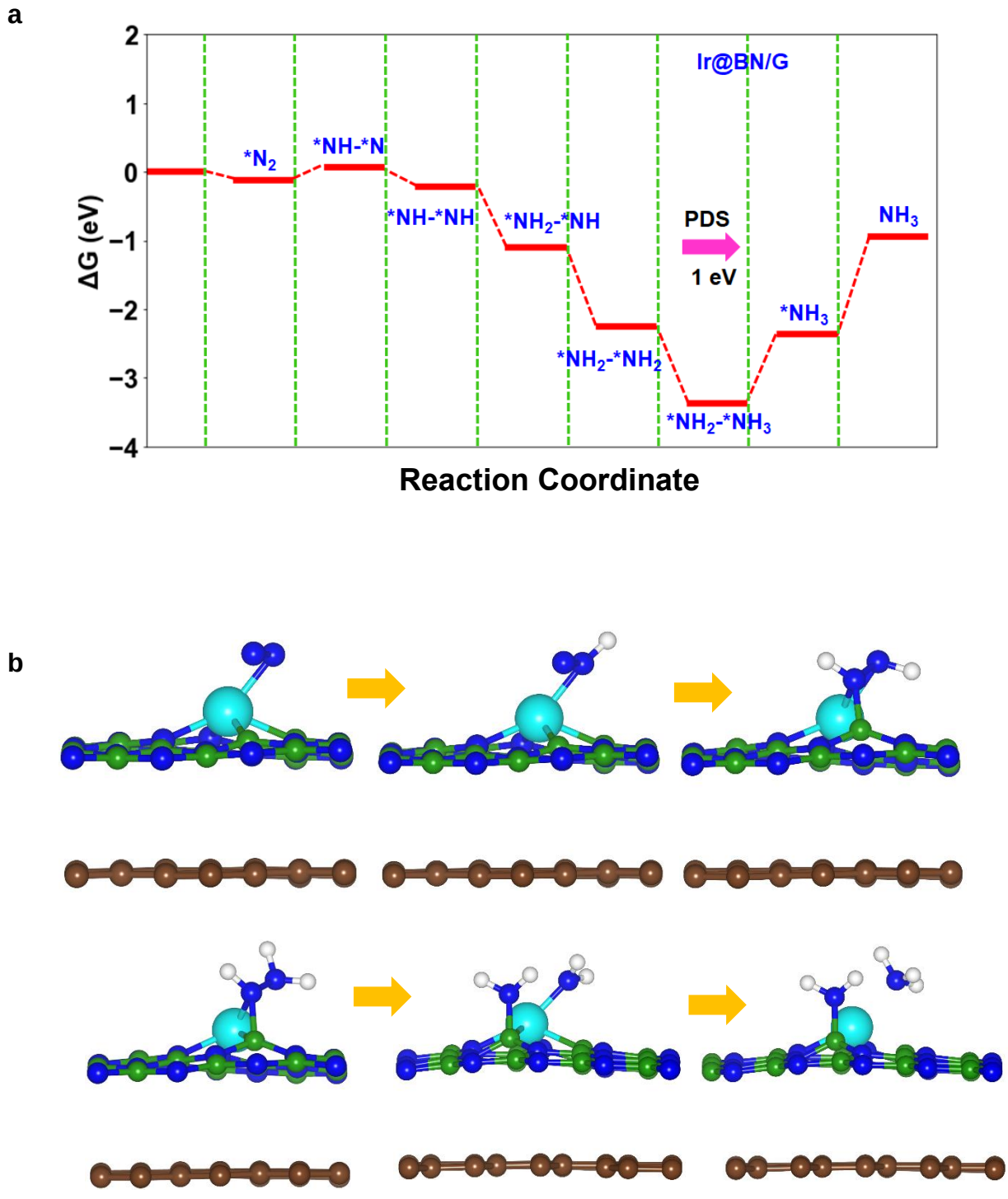

Figure S13. (a) Free energy diagram for N_2 reduction to NH_3 on Ir-doped BN/G SAC via enzymatic mechanism and (b) its adsorption structures during the NRR reaction.

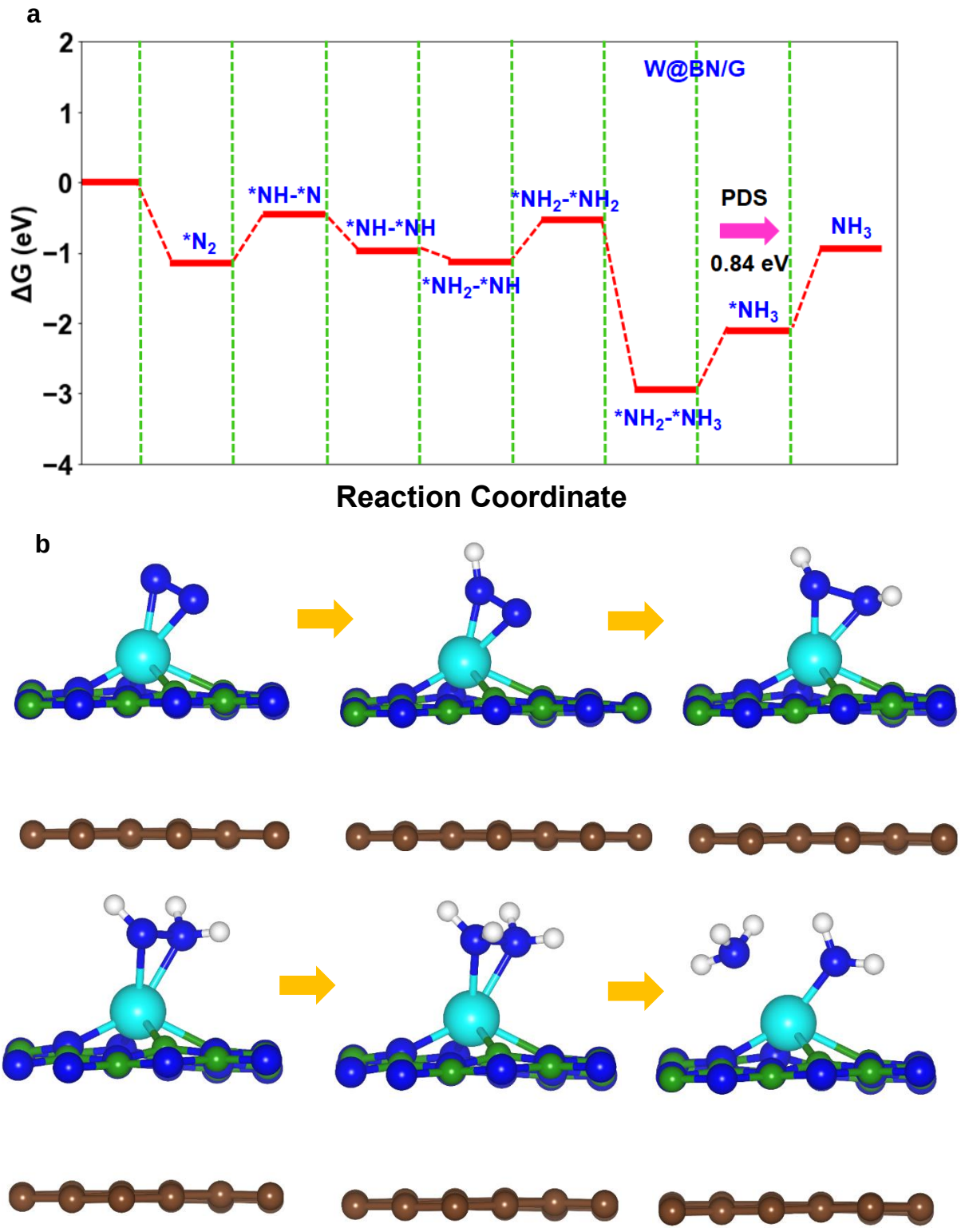

Figure S14. (a) Free energy diagram for N_2 reduction to NH_3 on W-doped BN/G SAC via enzymatic mechanism and (b) its adsorption structures during the NRR reaction.

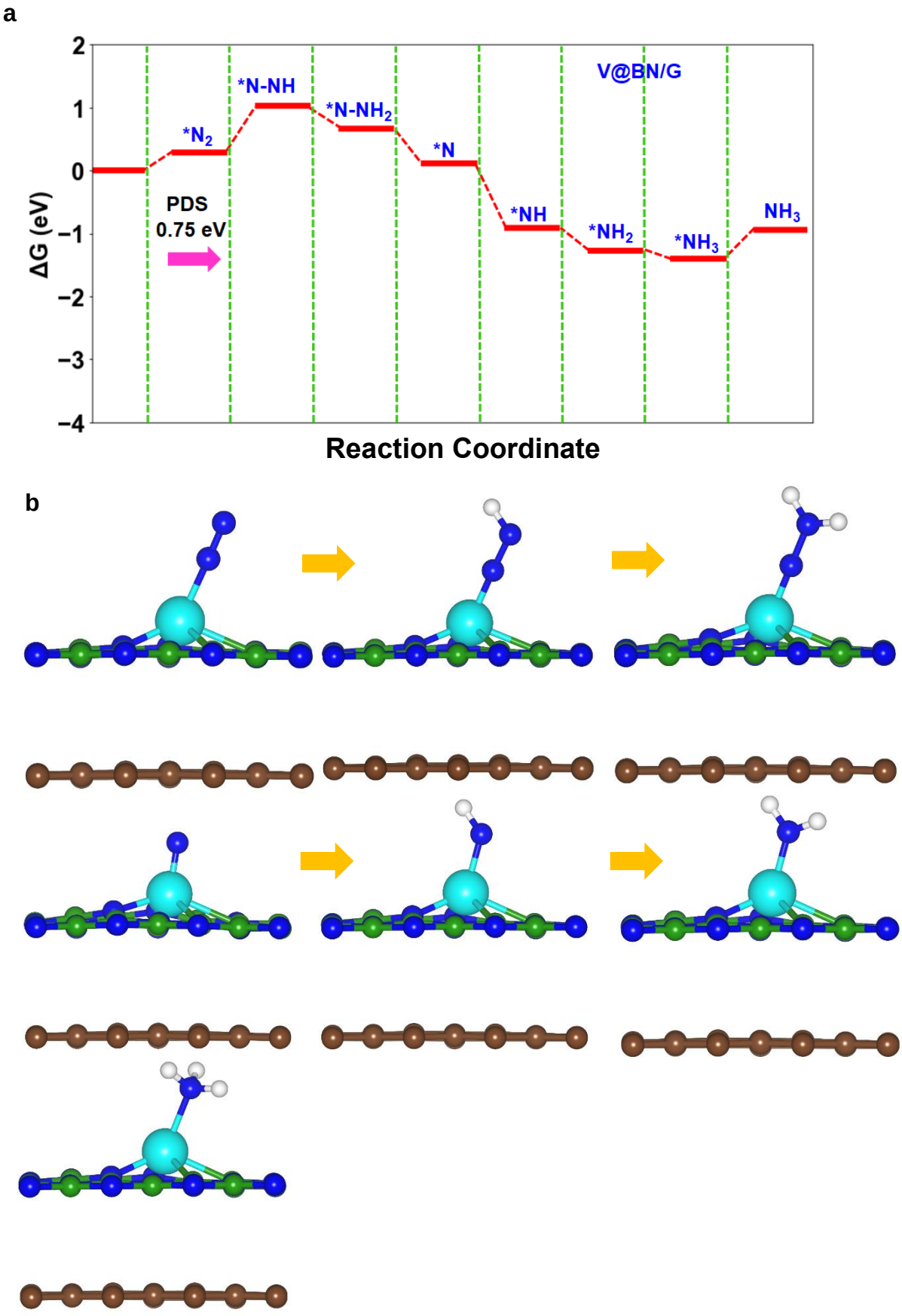

Figure S15. (a) Free energy diagram for N_2 reduction to NH_3 on V-doped BN/G SAC via distal mechanism and (b) its adsorption structures during the NRR reaction.

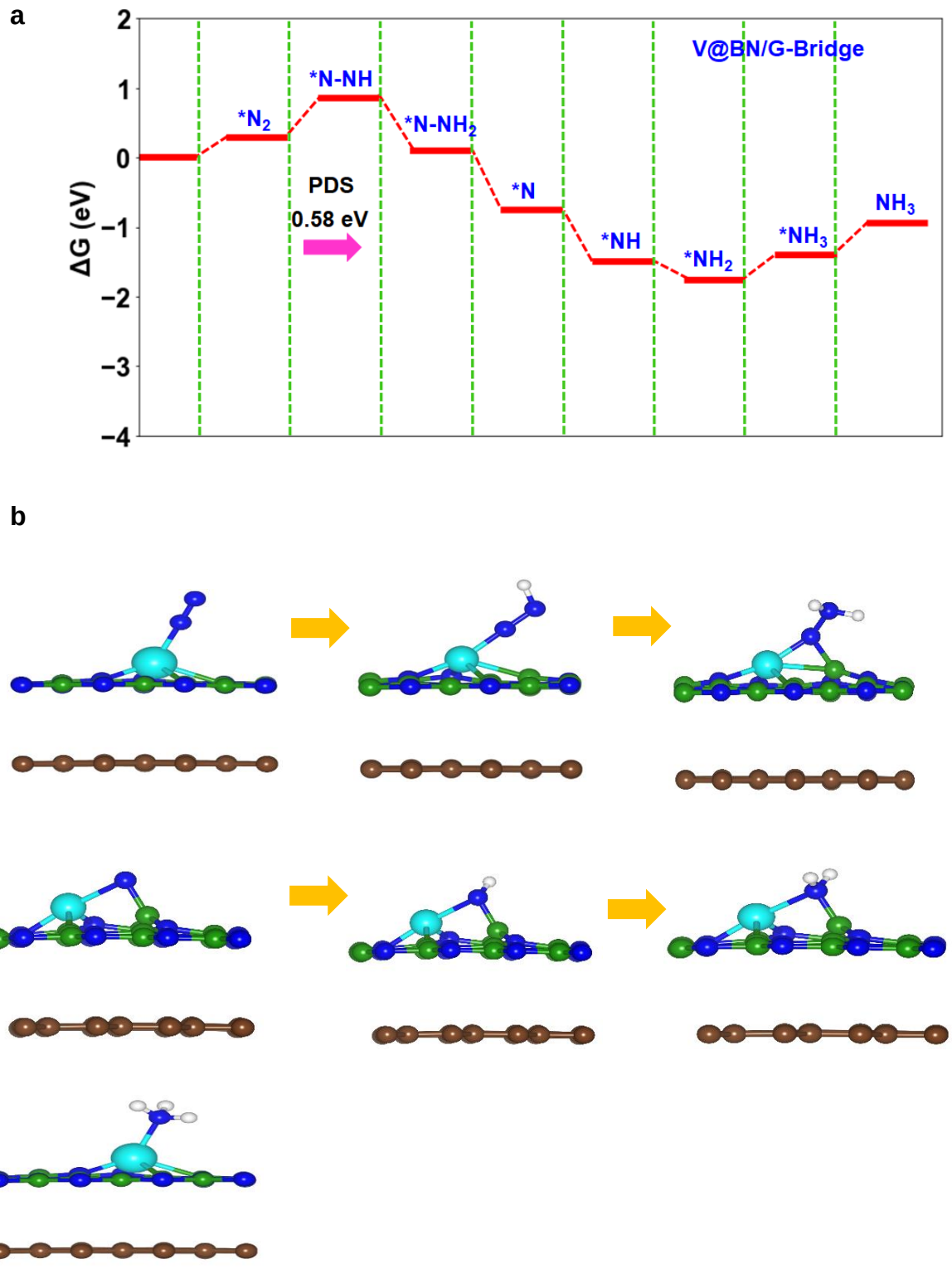

Figure S16. (a) Free energy diagram for N_2 reduction to NH_3 on V-doped BN/G SACs via distal mechanism (bridge site) and (b) its adsorption structures during the NRR reaction.

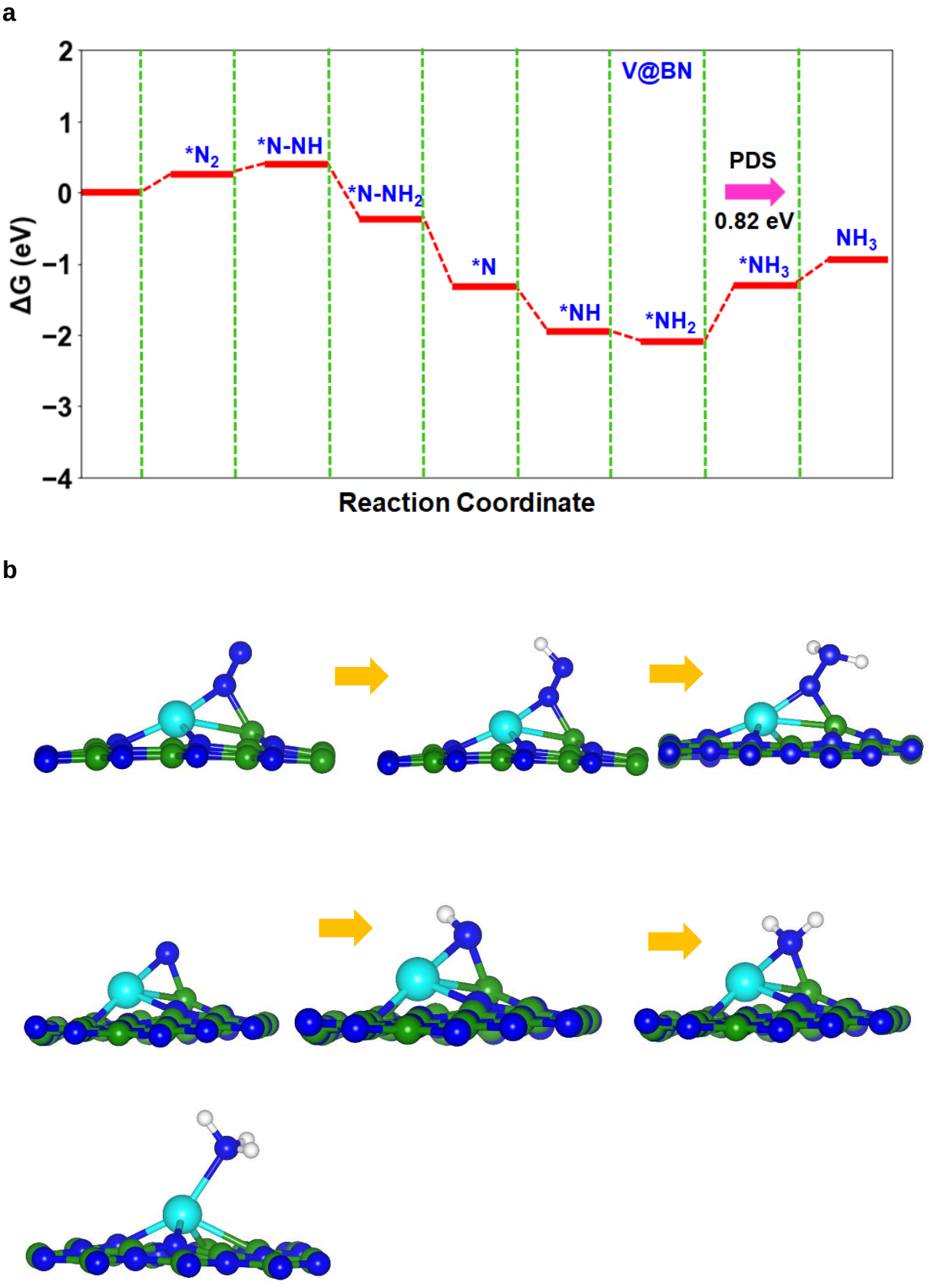

Figure S17. (a) Free energy diagram for N_2 reduction to NH_3 on V-doped BN SACs via distal mechanism and (b) its adsorption structures during the NRR reaction.

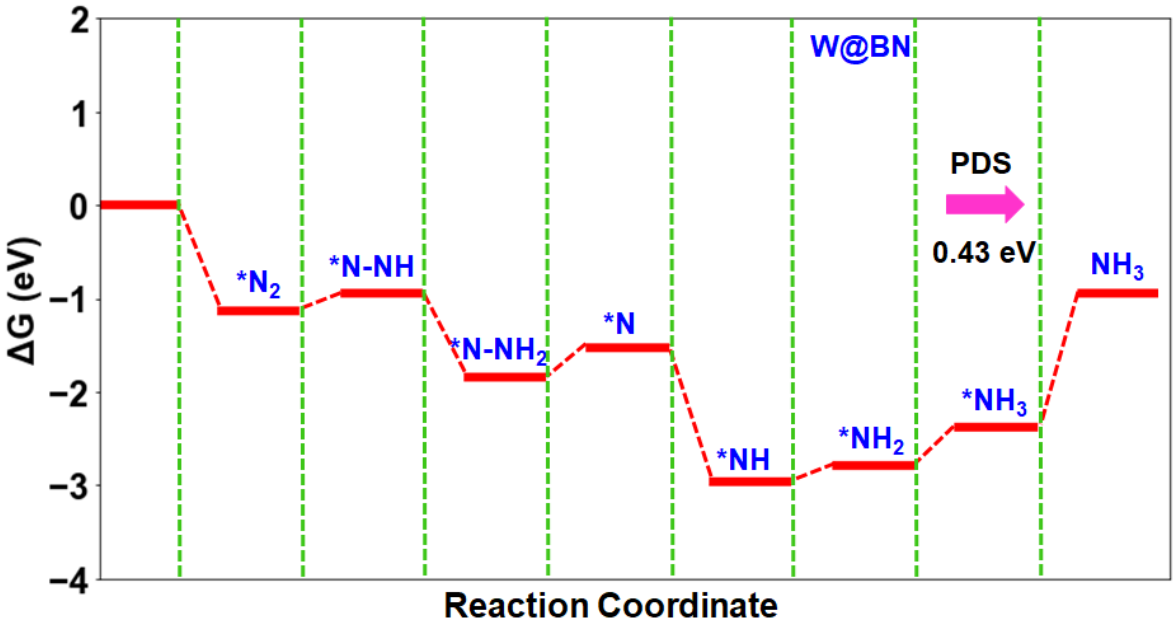

Figure S18. Free energy diagram for N_2 reduction to NH_3 on W-doped BN SACs via distal mechanism.

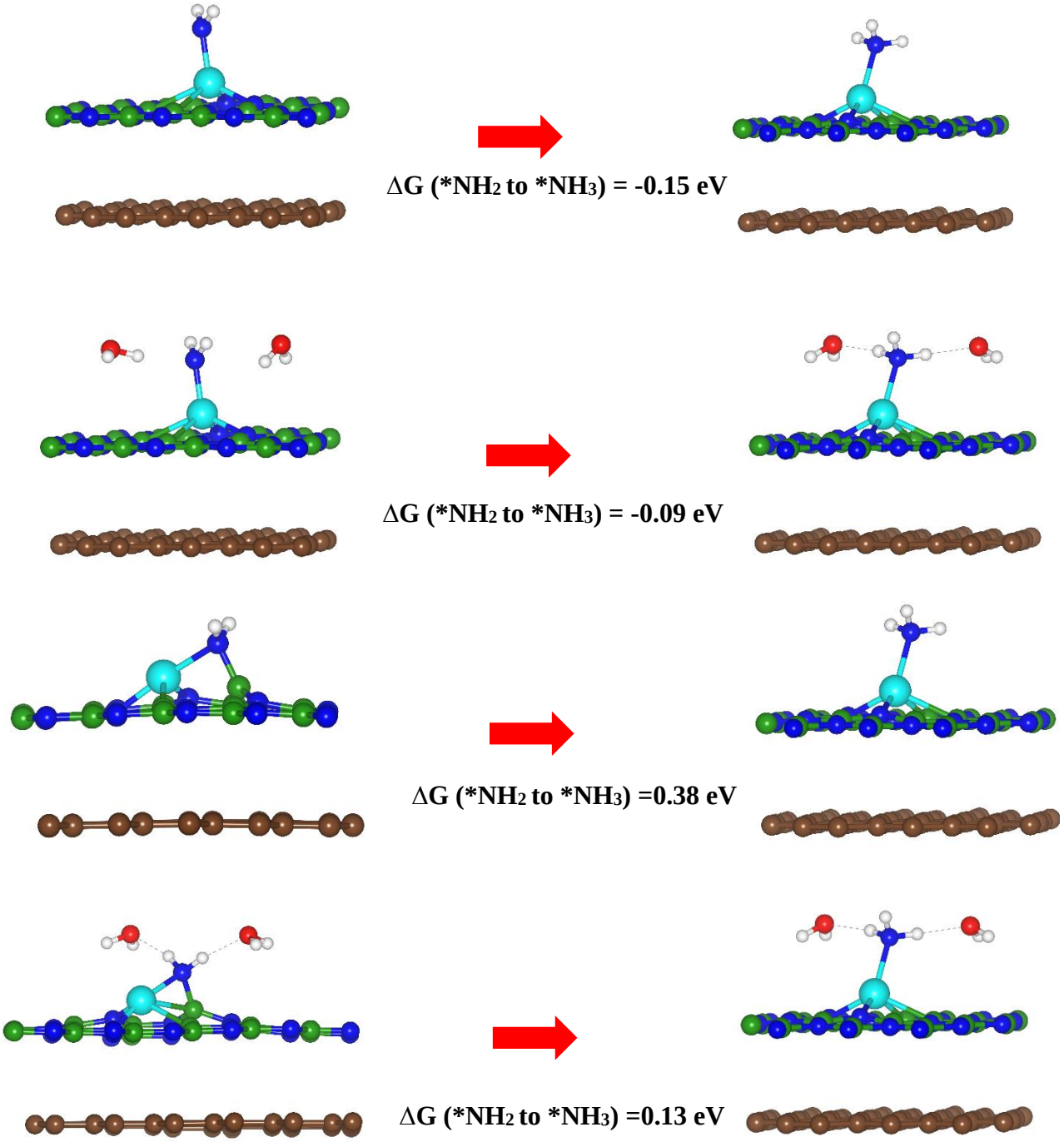

Figure S19. (a) Gibbs free energy for *NH_2 to *NH_3 elementary step employing implicit solvation model or a mixed implicit + explicit solvation model on V-doped BN/G SAC.

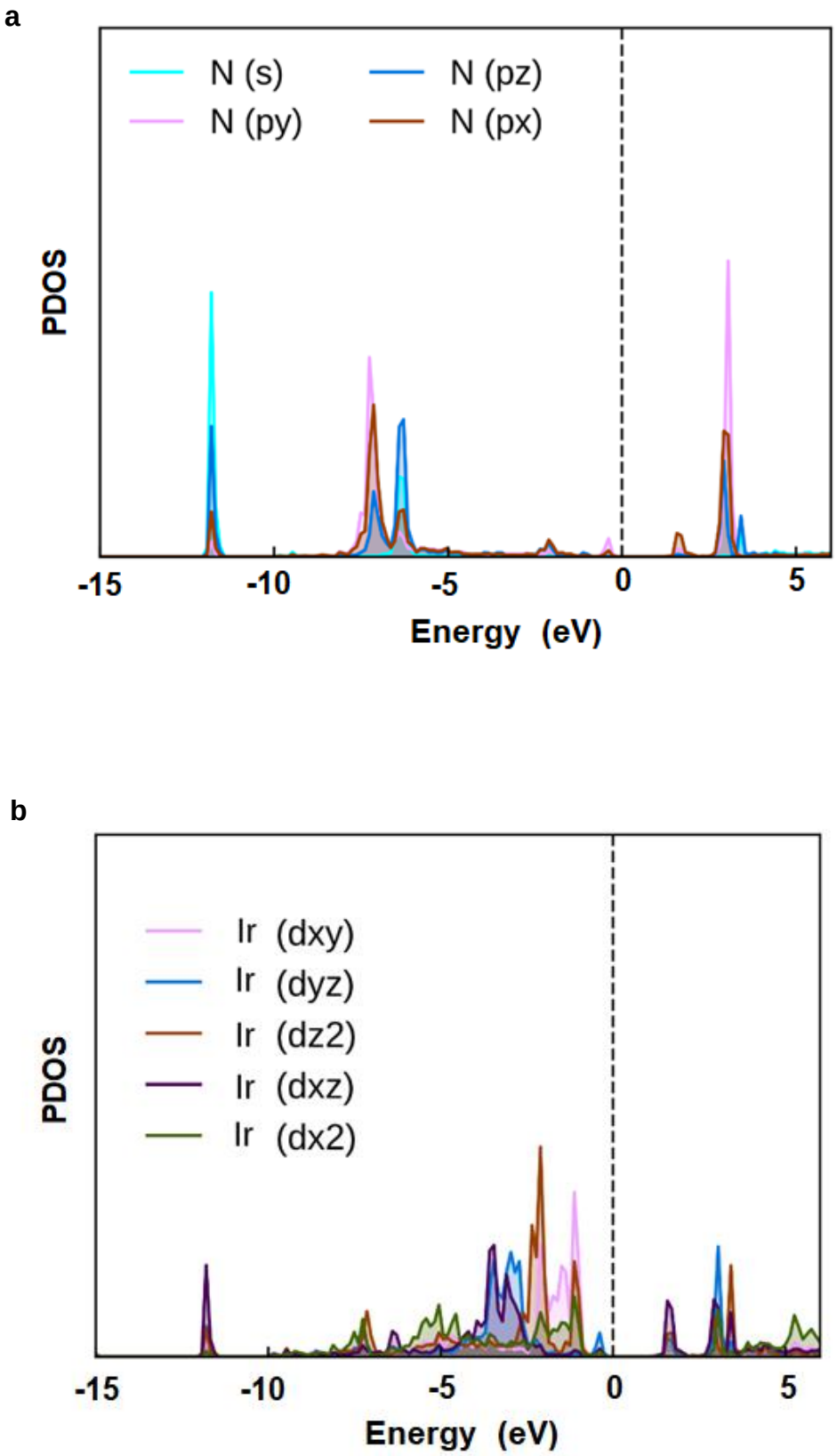

Figure S20. Projected density of states (PDOS) for (a) s and p orbitals of adsorbed N_2 and (b) d-orbitals of Ir on Ir-doped BN/G SAC.

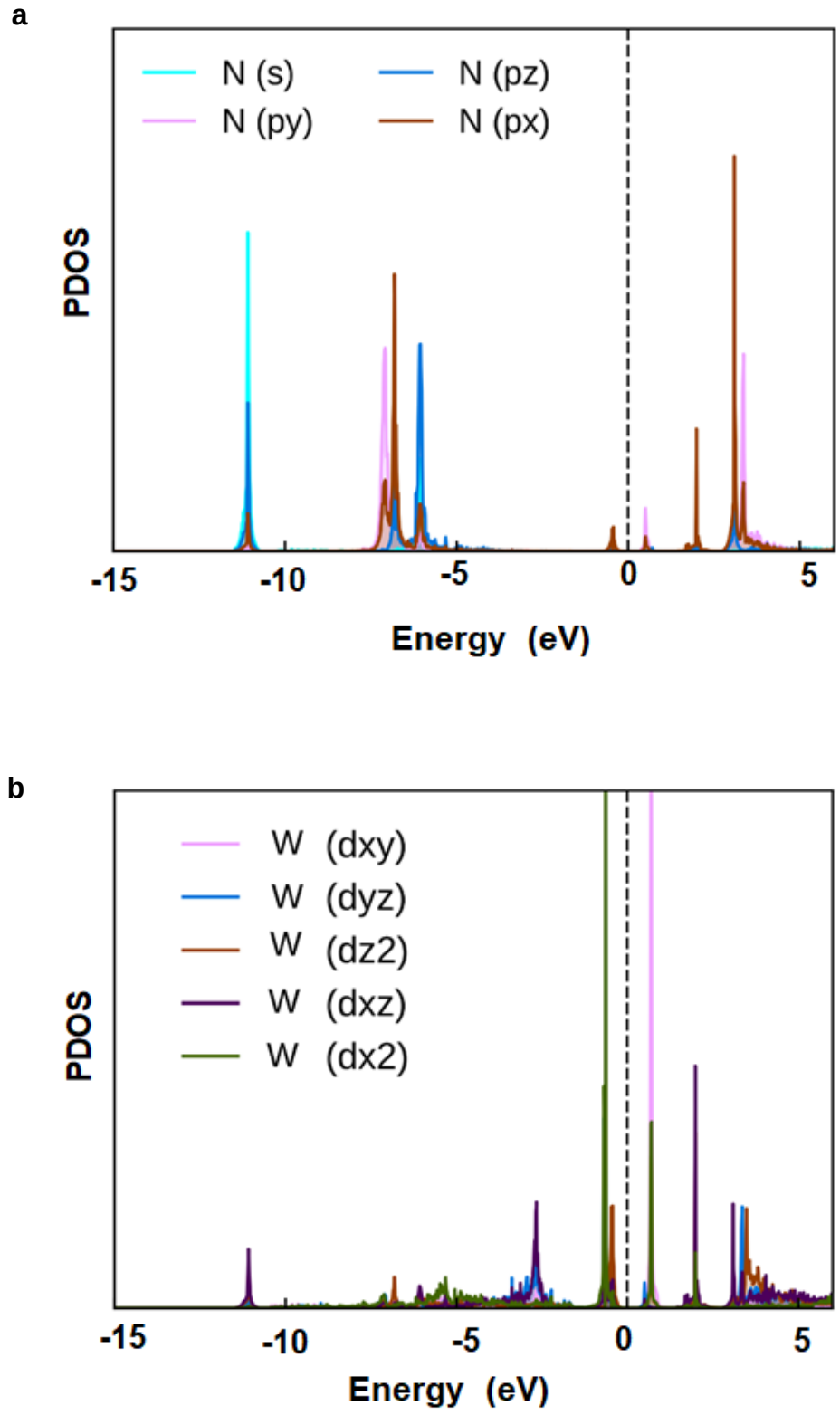

Figure S21. Projected density of states (PDOS) for (a) s and p orbitals of adsorbed N_2 and (b) d-orbitals of W on W-doped BN/G SAC.

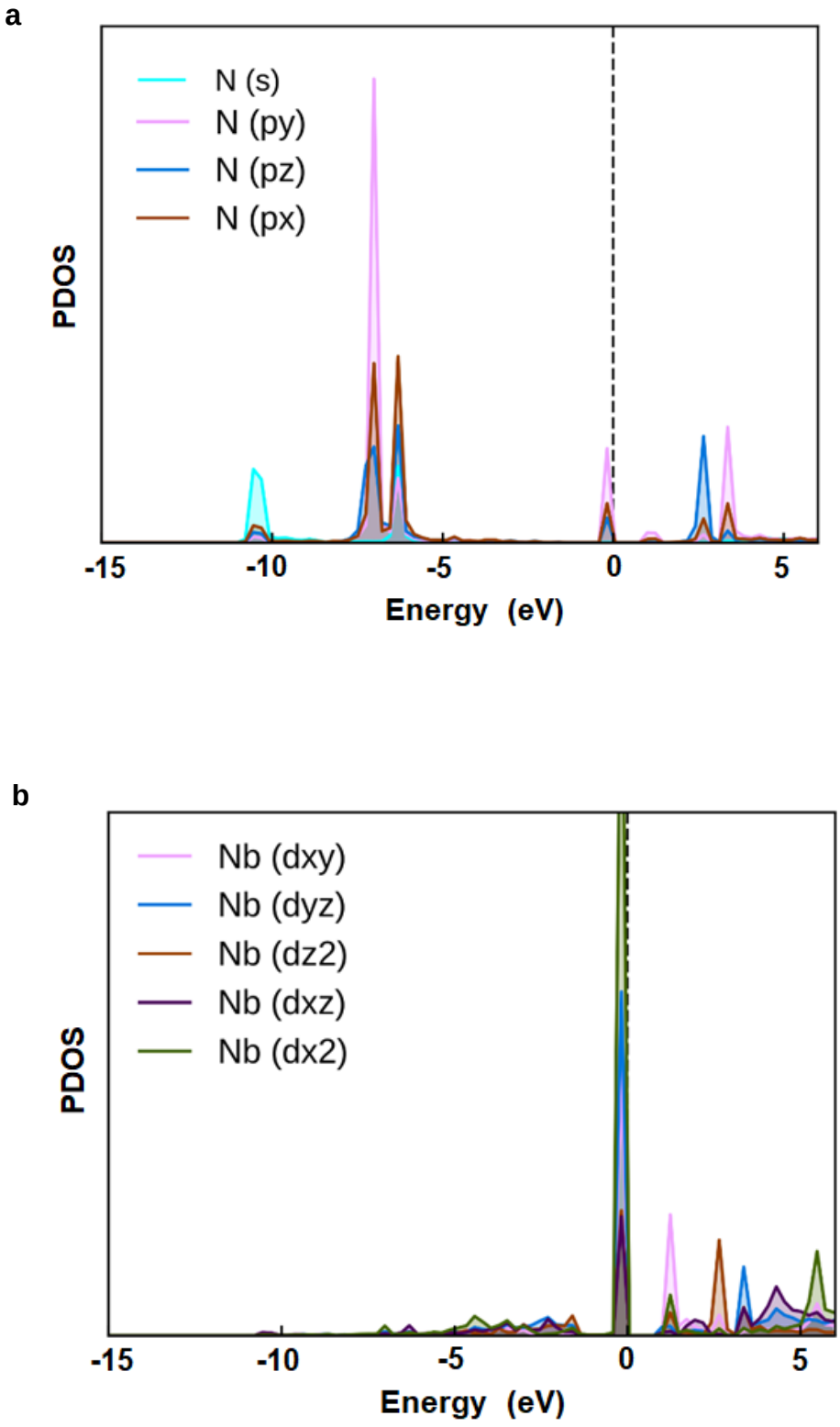

Figure S22. Projected density of states (PDOS) for (a) s and p orbitals of adsorbed N_2 and (b) d-orbitals of Nb on Nb-doped BN/G SAC.

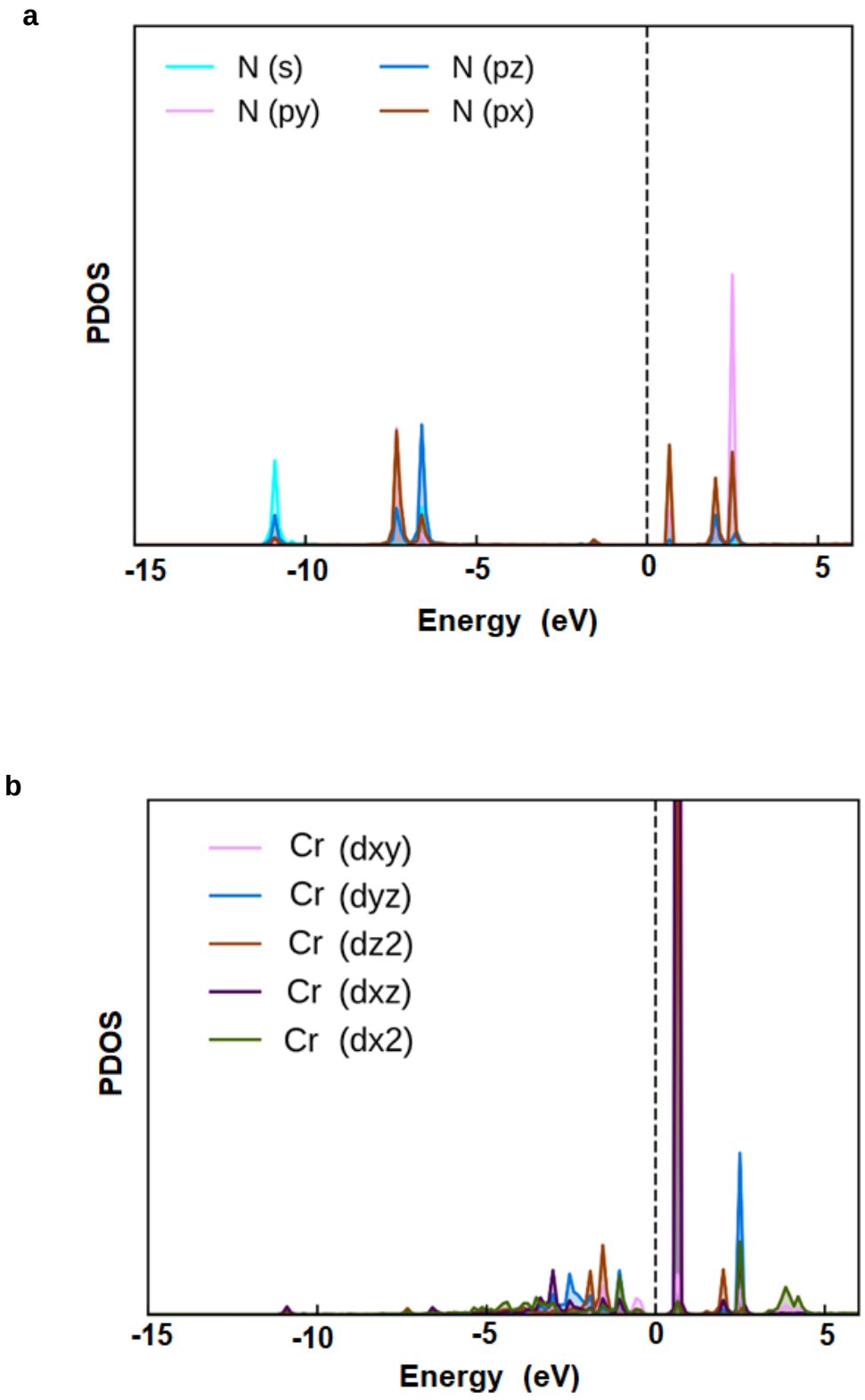

Figure S23. Projected density of states (PDOS) for (a) s and p orbitals of adsorbed N_2 and (b) d-orbitals of Cr on Cr-doped BN/G SAC.

Table S1. Magnetic moments of TM and its coordination environment (B_2N_2) on BN/G hybrid SACs.

Catalyst	TM (μ_B)	N1(μ_B)	N2(μ_B)	B1(μ_B)	B2(μ_B)	Total
W-BN/G	1.16	-0.01	-0.01	0.010	0.010	1.28
Mo-BN/G	1.23	-0.012	-0.012	-0.002	-0.002	1.29
V-BN/G	1.97	-0.033	-0.033	0.056	0.056	2.17
Cr-BN/G	3.17	-0.049	-0.049	0.024	0.024	3.24
Nb-BN/G	0.25	-0.005	-0.005	0.019	0.019	0.34

Table S2. Comparing potential determining step (PDS) of BN/G hybrid structures with some SACs in previous studies

Substrate	Active site	PDS (eV)	References
Boron-Nitride	Mo	0.35	*1*
Graphene	W	0.25	*2*
Nitrogen doped-Graphene	Mo	0.5	*3*
Nitrogen doped-Graphene	Ti	0.69	*4*
Boron-Nitride/G	V	0.22	*This study*
Boron-Nitride/G	W	0.41	*This study*

Table S3. Computed zero-point energy and entropy corrections at 298.15 K for different adsorbate species.

Adsorbate	ZPE (eV)	TS (eV)	Adsorbate	ZPE (eV)	TS (eV)
*N-N	0.2	0.18	*N-*N	0.2	0.13
*N-NH	0.43	0.12	*N-*NH	0.5	0.13
*N-NH_2	0.74	0.15	*NH-*NH	0.79	0.14
*N	0.08	0.06	*NH_2-*NH	1.12	0.14
*NH	0.34	0.14	*NH_2-*NH_2	1.45	0.16
*NH_2	0.63	0.11	*NH_2-*NH_3	1.75	0.2
*NH_3	1.02	0.13			

References

1. Zhao, J.; Chen, Z., Single Mo atom supported on defective boron nitride monolayer as an efficient electrocatalyst for nitrogen fixation: a computational study. *J. Am. Chem. Soc.* **2017,** *139* (36), 12480-12487.
2. Ling, C.; Ouyang, Y.; Li, Q.; Bai, X.; Mao, X.; Du, A.; Wang, J., A General Two-Step Strategy–Based High-Throughput Screening of Single Atom Catalysts for Nitrogen Fixation. *Small Methods* **2019,** *3* (9), 1800376.
3. Zhao, W.; Zhang, L.; Luo, Q.; Hu, Z.; Zhang, W.; Smith, S.; Yang, J., Single Mo1 (Cr1) atom on nitrogen-doped graphene enables highly selective electroreduction of nitrogen into ammonia. *ACS Catal.* **2019,** *9* (4), 3419-3425.
4. Choi, C.; Back, S.; Kim, N.-Y.; Lim, J.; Kim, Y.-H.; Jung, Y., Suppression of hydrogen evolution reaction in electrochemical N2 reduction using single-atom catalysts: A computational guideline. *ACS Catal.* **2018,** *8* (8), 7517-7525.